2022 44th Annual International Conference of
the IEEE Engineering in Medicine & Biology Society (EMBC)
Scottish Event Campus, Glasgow, UK, July 11-15, 2022

2022 44th Annual International Conference of the IEEE Engineering in Medicine & Biology Society (EMBC) | 978-1-7281-2782-8/22/$31.00 ©2022 IEEE | DOI: 10.1109/EMBC48229.2022.9870980

A System-on-Board Integrated Multi-analyte PoC Biosensor for Combined Analysis of Saliva and Exhaled Breath

Roslyn S. Massey
Dept. of Electronics
Carleton University
Ottawa, Canada
roslynmassey@cmail.carleton.ca

Bruno Gamero
Dept. of Electronics
Carleton University
Ottawa, Canada
brunogamero@cmail.carleton.ca

Ravi Prakash*
Dept. of Electronics
Carleton University
Ottawa, Canada
ravi.prakash@carleton.ca

***Abstract*— The need for oral health monitoring Point of Care (PoC) systems is ever growing. This is effectively highlighted by the ongoing COVID-19 pandemic where the lack of rapid PoC testing has placed an unsustainable burden on centralized laboratory testing. Urgent development has furthered pathogenic nucleic acid and antibody detection in oral samples throat swabs, but without corresponding advancements in biochemical monitoring through oral biosensing. We have recently reported two novel biosensor technologies for detection of high impact hormones: cortisol in saliva by organic electrolyte gated FETs (OEGFETs), and 8-isoprostane in exhaled breath condensate (EBC) using molecularly imprinted electroimpedance spectroscopy biosensors (MIP EIS). In this work, we report a first stage integration of the two biosensors — previously bench-top proven — with a miniaturized semi-hermetically sealed soft-fluidic enclosure, onto a low-power (<300 mW) customized printed circuit board. Our findings established comparable detection thresholds for the miniaturized board-based configuration and a lab-based test setup, and their ability to characterize, calibrate, and operate these small footprint biosensors. Testing with the 8-isoprostane EBC MIP EIS biosensors showed the system-on-board had an effective frequency range of 100-100kHz, comparable to lab bench impedance analyzers. Despite internal impedance increases of 210%, the expected data features are present in the impedance graphs collected with the PCB. The system-on-board experiments using OEGFET aptasensor showed a predictable behavior and comparable sensor detection range and resolution using unadulterated supernatant and serial dilutions of cortisol over a range of 273µM to 2.73pM. The portable, multi-analyte oral biosensor is a promising prototype for future packaging and clinical validation.**

Keywords—System-on-board integration, Organic electrolyte gated-FET biosensor, molecularly imprinted sensors, saliva testing, exhaled breath condensate, PoC device.

I. Introduction

Point of care (PoC) devices monitor certain biomarker and bio-signal levels at patients' bedsides, without healthcare personnel or benchtop instruments. Currently, electrophysiological bio-signals are monitored using PoC systems whereas only a few biomarkers extreme threshold levels are measured and used in clinical diagnostics. Two of these biomarkers are steroid hormone cortisol for diagnosing Addison's and Cushing's syndromes; and eicosanoid hormone 8-Isoprostane for oxidative stress and obstructive sleep apnea. Diagnostic cortisol levels are quantified through blood enzyme linked immune sorbent assay (ELISA) [1], whereas 8-isoprostane is measured through Gas or Liquid chromatography/mass spectrometry or ELISA analysis of blood [2]. Rapid, low-cost PoC devices would revolutionize biomarker usage beyond high threshold detection to trend analysis thereby improving the holistic understanding of associated diseases and preventative health monitoring. Presently, only two PoC biomarker quantification devices are in use — the Abbott i-Stat and the Siemens Epoc — both use blood as the bio-fluid. Blood most accurately captures patient biomarker levels but requires phlebotomy, increasing patient risk and relegating the devices to a hospital or centralized laboratory.

Novel experimental PoC devices focus on non-invasive analytes such as saliva, exhaled breath, sweat and urine to overcome the limitations of blood-based analysis. The two most promising analytes are saliva and exhaled breath. They can be collected non-invasively during activity or in repeat testing environments, possess greater biomolecule target variety and reliability than urine, and have fewer risk factors for phlebotomist and patient than serum [3,4].

Saliva is called the 'mirror of the body' as it contains a vast biomarker array with predictable, repeatable correlations to serum [5]. Salivary hormone concentrations are usually 1-8% of serum concentrations, requiring highly sensitive quantification [4,7]. For example, the salivary concentration of the steroid hormone cortisol is 7-80 nM compared to serum at 138-635 nM [8]. Therefore, an effective saliva biosensor must be accurate, precise with a low Limit of detection (LoD) despite complex media content and variability.

Organic Field Effect Transistor (OFET) biosensors have a desirable facile nature, low-cost, large area processability, and flexible form factor [9]. Incorporating electrolytes directly into the OFET's gate dielectric means electrolyte composition directly effects output characteristics – the established sensing mechanism for our organic electrolyte gated FET (OEGFET) biosensors [10-12]. Furthermore, our

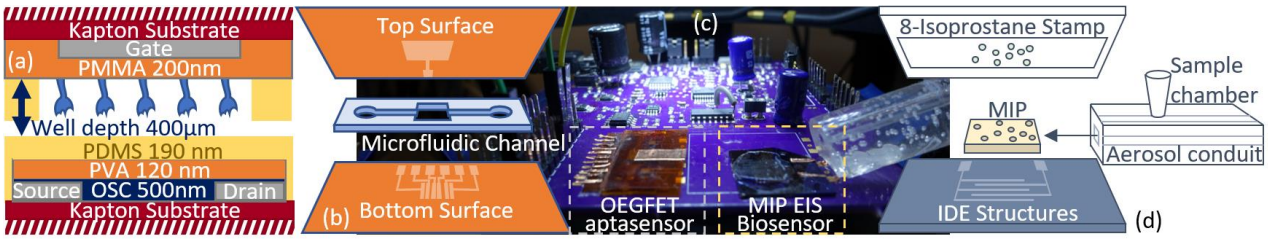

Fig. 1. (a) OEGFET Aptasensor graphical representation of cross section, (b) OEGFET aptasensor two surface device with integrated Microfluidic channels, (c) Devices under test, (d) MIP EIS biosensor basic set up and aerosolization method.

label-free OEGFET aptasensor implementation minimizes the integration challenges posed by traditional electrolyte gated OFETs by physically isolating the gate and OSC from the electrolyte using ultra-thin polymer dielectric layers [11]. Aptasensors possess beneficial attributes of fast turn on, biomolecule selectivity, reusability, and stability which we have demonstrated for detecting cortisol in spiked saliva supernatant solutions. The unique integration of the soft-fluidic microchannels and the facile testing process of the OEGFET aptasensor renders it promising as a PoC device provided it can be integrated with a data acquisition setup.

Exhaled breath (EB) is another promising oral bio-fluid for PoC application. EB analyzers target volatile organic compound (VOC) biomarkers and endogenous non-volatile biomaterials. VOC EB analysis has been a commercial success with IR spectroscopy and gas chromatography [13], however, PoC devices cannot implement these techniques due to high power and testing requirements [14]. Despite VOC analysis success there are no validated commercial EB PoC tests for non-volatile materials. Non-volatile biomarkers rely on lab bench analysis of EB Condensates (EBC) [15-16]. Impedance and metal-oxide semiconductor (MOS) detect EB non-volatile materials with good sensitivity, but often poor selectivity and stability [17]. Given the media complexity, low concentrations, and small signal to noise ratios, this is a significant limitation [18,19]. We recently proposed a soft-lithography Molecularly Imprinted Polymer (MIP) based electroimpedance spectroscopy (EIS) biosensor which produces a novel low-cost, fast (<1 minute), robust, analysis of stress hormone, 8-isoprostane [20,21]. MIPs are called plastic antibodies, as the process of imprinting biomolecules on polymers creates low energy binding sites for repeat testing, offering comparable selectivity and sensitivity to antibody-based sensors, but with a simpler fabrication and improved durability [22,23]. MIP sensors are robust to temperature, humidity and pH changes that confound other sensors [24]. Literature examples of MIP EB and EBC sensors also show efficacy for detecting complex bacteria, small biomolecules, and VOC sensing [21,25,26].

In this work, we demonstrate for the first time a multiplexed oral bio-analyte sensor system, configured to operate using a USB powered small footprint printed circuit board, to detect highly specific hormone biomarkers from saliva and EBC (Fig. 1c). We investigated the performance of our board-based multi-analyte biosensor by comparing the efficacy of our PCB data collection in reproducing gold standard lab instrumentation-based data collection methods. The system on board predictably reproduces our OEGFET aptasensors inverse concentration to output current correlation using blank saliva supernatant and cortisol spiked supernatant in the range of 2.73 pM – 273 µM. The board-based system has an effective frequency range comparable to lab bench devices of 100-100 kHz. The impedance graph features are reproduced in the PCB data despite an 210% increase in impedance, making this a promising first step towards a fully portable, low power (<300 mW) small footprint multianalyte sample to analysis device. Our current device is a preliminary prototype, demonstrating the feasibility of a fully portable, non-invasive PoC biosensors with fast, accurate, and repeatable performance.

II. Materials and Methods

A. Materials

The OEGFET aptasensor was fabricated on polyimide (Kapton®, Dupont USA) flexible substrates (Fig. 1a). 6,13-Bis(triisopropylsilylethynyl) pentacene (TIPS-pentacene) (Sigma Aldrich, USA) is solution processed as 1 wt. % in chlorobenzene (Sigma Aldrich, USA). Poly (vinyl Alcohol) (PVA), Poly (methyl methacrylate) (PMMA) (Sigma Aldrich, USA) and Sylgard 184 polydimethylsiloxane elastomer (PDMS) (Dow Chemicals) are used for device structure and dielectrics. (3-Aminopropyl) triethoxysilane (APTES) (Sigma Aldrich, USA) binding processes are used to adhere incompatible materials. For creating the MIP sensor, Poly(vinyl-alcohol), N-methyl-4(4'-formylstyryl) pyridinium methosulfate acetal (PVA-SbQ) (13.3 % solution in water) was purchased from Polysciences Inc. (USA), whereas the 8-isoprostane was purchased from Cayman Chemical (USA), for synthetic addition to EBC using the fluidic aerosolization channel (Fig.1d).

B. Sensor Fabrication

1) MIP EIS Sensor

A soft lithography stamp was prepared by dropping 50µg of 8-ISP in 50µL of DI water onto a 0.5cm^2 PDMS surface cured on glass and dried at 37°C for 45 minutes. 250nm PVA-SPQ was spun onto chromium (Cr) on silicon interdigitated electrodes (IDEs). The soft lithographic stamp was then placed onto the uncured PVA-SPQ, and UV cured (365nm light, 30 minutes). Removing the stamp was

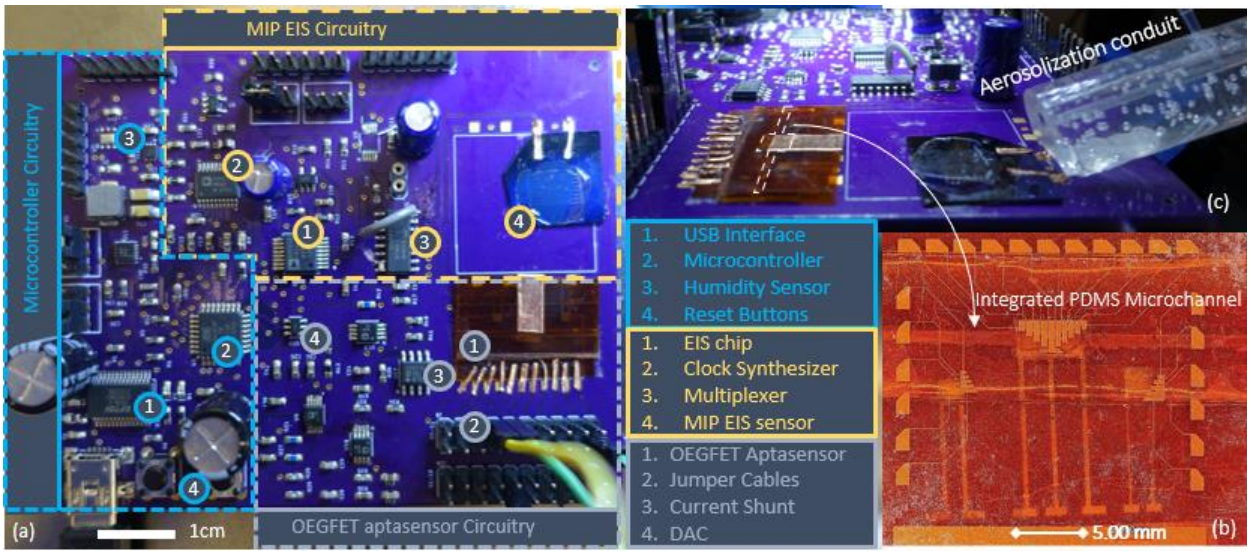

Fig. 2. Images of (a) PCB layout identifying key circuit components, (b) OEGFET aptasensor with integrated microfluidics for handing saliva samples, photographed through the bottom surface, (c) MIP EIS biosensor device under test showing the microfluidic aerosolization conduit for the EBC sensing.

followed by a DI water wash to remove any adhered 8-isprostane and uncured PVA-SBQ. The PVA-SBQ layer is label-free, specific to 8-isoprostane and reusable. This provides the functionality to the MIP EIS biosensor. The aerosolization tube was prepared by curing PDMS around a 2 mm diameter air intake channel. A small sample chamber synthesizes EB by aerosolizing small volumes (5 µL per test) for transport to the MIP EIS biosensor. Synthetic EBC is produced using the spiked 8-isoprostane in DI water solution. Varying EBC concentrations were attained by serial dilution of a 1 mg/mL stock solution, down to 1 pg/mL 8-isoprostane as EBC.

2) OEGFET Aptasensor

The bottom source-drain transistor electrodes are printed on Kapton® using conventional lift off techniques, of 50 nm aluminum (Al) and 150 nm Cr. The surface is UV Ozone activated with a Technics plasma cleaner. 500 µm of TIPS-pentacene, 120 nm of PVA and 190 nm of 10:1 elastomer to curing agent PDMS are spin deposited. PDMS is left uncured for the final integration step [12]. The PDMS microchannels are cast in a 3D printed mold with a testing well depth 0.4 mm and cured. The Kapton top surface has a 200 nm Cr shadow mask deposited top gate and a 200 nm layer of PMMA. The PMMA and PDMS microchannels are adhered by APTES crosslinking suited to our low temperature process [11]. Aptamers are immobilized by drop casting onto the UV activated PMMA surface [12,27]. The final step contacts the PDMS microfluidic channel with the uncured bottom surface PDMS layer and cured at 21°C for 72 hours (Fig. 1b). The result is a soft-fluidic integrated OEGFET aptasensor with flexible micro-channels for handling spiked saliva supernatant samples.

Saliva was collected via passive drool and centrifuged (6000 rpm, 30 mins). The spiked supernatant is 50ml of the blank decanted supernatant (RSNB) and 50µg cortisol to produce a 2.73µM cortisol in saliva solution (RSN1) and a dilution series down to 2.73pM (RSN7).

C. PCB Integration of the Two Biosensors

A custom PCB, shown in Fig. 2a, was designed to control both the EIS and I-V sweeps during the board-based testing. The system-on-board is powered by a USB with a 5 V control voltage and has a 12 MHz clock. It consumes a max power of 300 mW while operating both sensors. To achieve the fast response rate for the biosensors (<1 ms), stabilizing time between tests was regulated to 10 ms. The on-board network analyzer performs the impedance analysis and returns real and imaginary impedance components. The signal is attenuated using external resistors to allow for measurement below 1 kΩ. The attenuation and subsequent 2.5 V offset are acceptable for the common mode set up. A direct digital synthesis (DDS) is used as a variable clock generator due to the high frequency range. The Atmega328 microcontroller runs the OEGFET aptasensor I-V sweeps for testing and calibration. The 5 V output of the DAC is amplified by a factor of 1.2 to reach the 0-6 V sensor biasing requirement. The drain current, passed through a 20 Ω drain resistor, is amplified, and measured by a AD8210 current shunt to output an amplified proportional voltage to sensed current. An ADC then sends the result to the microcontroller to output. The multiple aptasensor transistors are accessed through low impedance jumpers for simple testing of multiple devices without the use of a multiplexor. The four MIP EIS biosensor locations are for future integration of peripheral sensors such as humidity, temperature, and a reference EIS sensor.

D. Testing and Validation

1) MIP EIS Biosensor

EBC spiked with 8-isoprostane was used to demonstrate the efficacy of the biosensor. DI water was used as a

negative control to compare results. 5µl of each 8-isoprostane in DI water sample were aerosolized on the MIP-EIS sensor over 60 s. The surface stabilized for 60 s, and then the readings are taken. The sample is cleaned with alcohol between each test to remove any bound 8-isoprostane. The lab bench impedance data was collected with an Agilent 4294A impedance analyzer with the 42941a impedance probe kit at room temperature, in a frequency range of 0.1 to 100 kHz. The PoC compatible electroimpedance data was collected using the previously described PCB based setup. The microcontroller calibrates the data for temperature, and then runs an impedance sweep over 0.1 to 100 kHz. This data is reformatted with an excel visual script to convert impedance to real and imaginary components. The Nyquist plots were generated, then analyzed in MATLAB.

2) OEGFET Aptasensor

10µL of spiked saliva supernatant was injected into the aptasensor microchannel for each test. 1x TAE buffer was used as the negative control reference between each sample, followed by a DI water rinse. The lab bench data is collected using a HP 4155A semiconductor parameter analyzer (SPA). Current –Voltage (IV) sweeps were performed by keeping a constant source drain voltage (V_{SD}) of 3V and sweeping the source gate voltage (V_{SG}) from 0 – 6V in increments of 12.5mV with a settling time of 500ms. The voltage range was established in our previously published OEGFET aptasensor works [12]. Our Source Current (I_{SD}) and leakage current (I_{GS}) data were collected for each test. Aptasensor PoC compatible tests are run by using the PCB-based setup where I-V sweeps using a V_{SD} of 3V and a V_{SG} sweep of 0-6 V are performed by the ATMEGA328 microcontroller. Current values for the two sweeps are averaged over the linear range of the voltage sweeps, established as V_{SG} 3.3-3.8 V. This gives a realistic representation of the resolution between concentrations. Device capacitance is extracted from the I-V sweeps using the modified Marinov Model for OFET devices and the MATLAB Curve fitting tool.

III. Results and Discussion

A. MIP EIS Biosensor Performance with Spiked EBC

The MIP EIS biosensor impedance response is characterized by an equivalent circuit model as shown in figure 3c. The contact resistance (R_C) is a factor of coating material and solution composition. The complex double layer capacitance is approximated as a constant phase element (CPE_{DL}) with a similar impedance to a capacitor, but with phase change α. Surface resistance R_S and IDE geometry-based capacitance (C_G) are extracted as parameters of interest. After identifying the high corner frequency of the Nyquist plot, it calculates the semicircle radius (figure 3b). The x intercepts of the semicircle represent the R_C and R_C+R_S, Eqns. (1) and (2) are used to extract the C_G and C_{PEDL}, with the tail slope used to determine α. The peak frequency value is used to determine C_G, the geometry capacitance.

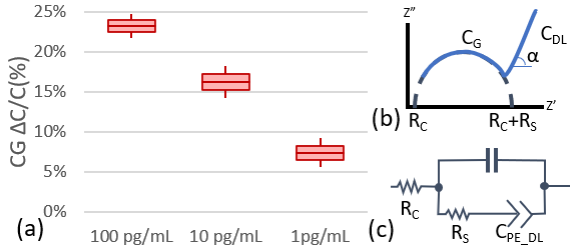

Fig. 3. (a) Box plot showing correlation between extracted C_G and 8-isoprostane concentration for MIP EIS biosensor, (b) Nyquist plot extraction process (c) MIP EIS equivalent circuit model.

$$C_G = \frac{1}{\omega_{peak} R_S} \quad (1)$$

$$C_{DL} = \frac{1}{\omega |Z|} \quad (2)$$

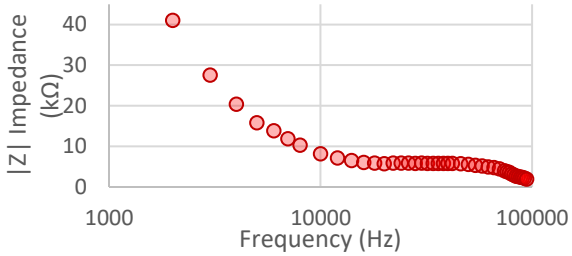

Fig. 4. Electroimpedance spectral (EIS) data sample extracted using the board-based setup utilizing the MIP biosensor

The MIP EIS biosensor data demonstrated the expected decrease in capacitance with decrease in concentration, indicating that our verified technology is functioning as expected. Fig. 3a shows the relationship between concentration and C_G. The MIP acts as a transducer as 8-isoprostane binding changes the coating surface energy, decreasing the C_G in a predictable repeatable fashion.

When moving to the PCB device, the first observation is that the expected impedance pattern is captured (Fig. 4). The data demonstrates a smooth integration across the three different clocks required to perform a sweep from 100-100kHz, a comparable range to lab bench impedance devices. The blank MIP EIS biosensor data had an increase in C_G between the impedance analyzer and the PCB of 210%. This increase is due to the internal impedances of the PCB board. The requirement for PoC devices is small, light with low voltage and current requirements. The power source and power delivery network are limited by the PoC requirements, but further optimization of impedance matching and limiting the parasitic capacitance will improve further prototypes of the PCB board. However, as the C_G data is extracted from the |Z| values, the preserved shape indicates the PCB is capturing the key capacitive behavior. Importantly, the impedance increase is consistent, indicating that though the background impedance is increased, the precision remains. The ability to run 4 MIP EIS biosensor devices from the same board allows for future integration of humidity, temperature and reference EIS devices for improving the PCB repeatability for future works. The

internal impedances of the board can be further optimized to increase the signal to noise resolution, leading to an effective platform for extracting impedance data.

B. Validation of Board-based OE GFET Aptasensor with Spiked Saliva Supernatant Samples

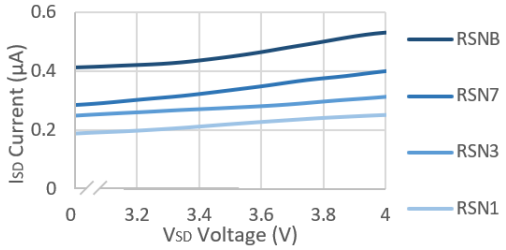

Fig. 5. Board extracted linear range OEGFET aptasensor data for dilutions of cortisol from blank supernatant (RSNB) to spiked supernatant samples, starting with 2.73 μM cortisol (RSN1).

The OEGFET aptasensor operates in the linear region of the characteristic current-voltage curves. The predictable change in output current for applied voltages in this region is directly correlated to the aptasensor gate capacitance. The aptasensor behavior is best described using the modified version of the Marinov model, which is used for extracting the lumped capacitance term c_{DI}. Our modified version is tailored for extracting data in the linear region, simplifying the extraction process removing extraneous parameters.

The biorecognition binding takes place in the electrolyte layer, accounted for in the modified Marinov model by changes in device capacitance, c_{DI} (3). The biosensing mechanism of action is fully described in our previous papers [10-12]. The collected data was digitally filtered to remove high sources of noise in MATLAB, and extraction of capacitance and power law dependence (m) values were extracted using the MATLAB curve fitting tool.

$$I_{ModMar}^{gen} = \frac{\mu_o}{V_{aa}^{1+m}} c_{DI} \left(\frac{W}{L}\right) V_{SD} (V_{SG} - |V_T|)^{2+m} \qquad (3)$$

Testing with Lab bench equipment identified the output characteristic linear region as a source drain bias V_{SD} range of 3.3-3.8 V for a V_{SG} of 3V. Gate leakage was monitored in all tests, producing a signal to noise ratio (SNR) between 10^2-10^3. The OEGFET aptasensor showed cortisol concentration dependent I_{SD} modulation as established in our previous work, where decreasing target analyte concentration increases device output current. The observed behavior is caused by aptamers complexing with cortisol introducing new terms into the capacitance mechanism [10-12]. This creates the inverse correlation between sample cortisol concentration and output characteristic that is ideal for low concentration (nM physiological range) materials such as salivary cortisol. Testing with the PCB in the linear region of the OEGFET aptasensor demonstrated cortisol concentration dependent I_{SD} modulation across the linear range (Fig. 5).

Figure 5 shows the PCB has reproduced the OEGFET aptasensor inverse concentration to output current and c_{DI} correlation, even with a complex media such as saliva.

The change in capacitance with concentration is linear over the physiologically relevant range, with a LoD comparable to literature examples of OFET biosensors (supernatant spiked with 2.73 pM cortisol compared to literature values of 0.8-1 pM) [28,29]. The OEGFET aptasensor with the PCB analysis has a predictable current to concentration response over the reported physiological range of cortisol in saliva of 30.7-323.9 nM [30]. The OEGFET has clear distinctions between tested concentrations demonstrating that this PCB board set up is compatible with a future PoC device.

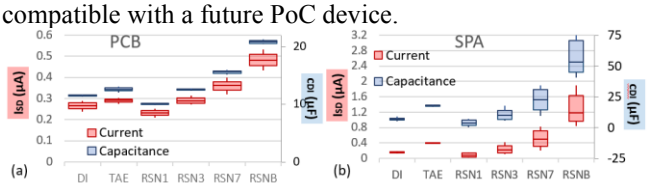

Fig. 6. Box plots illustrating (a) capacitance and aptasensor output current vs. cortisol concentration collected with the system-on-board setup, and (b) capacitance and current vs. concentration data collected with the SPA.

The OEGFET aptasensor is designed as an amperometric sensor where gate capacitance change is solely caused by cortisol binding to aptamers. Figure 6 shows boxplots of the output currents and extracted capacitances. Figure 6a shows the data collected with the PCB, and 6b the data collected with the SPA. The extracted c_{DI} values have less variation than the current values, an expected behavior from our established OEGFET aptasensor, and mimic the trend of the output currents. The PCB integrated OEGFET aptasensor has a predictable, characteristic relationship between the concentration and the I_{SD} and c_{DI}. Our simple voltage divider measurement set up functions as a sensor controller. However, the PCB data not only has reduced current values, but a decreased current range. The narrow PCB current and capacitance range compared to the SPA indicates the PCB sensitivity is lower than the lab bench SPA, and the reduced resolution makes the data more susceptible to noise. The decrease in sensitivity and resolution was anticipated as data is captured with a simple current shunt monitor with a total referred to output (rTo) error of 740 μV. As the collected data was in the 0-100 mV range, SNR was therefore affected by the rTo error. To mitigate this, each data set was allowed to stabilize before sensor response was collected, but observable ripple remained. The voltage ripple indicates that digital or analog filtering is required for the signal and voltage sources in the next phase of system-level integration to produce stable, repeatable measurements. Further optimizing the ADC will avoid sampling phenomena that introduce random error into the I-V curves. Future prototypes of the integration board would focus on improving sensor resolution by decreasing these noise sources throughout the board design.

IV. CONCLUSION

We have demonstrated a multiplexed portable PCB-based multianalyte sensor system for label-free quantification of cortisol and 8-isoprostane in two non-

invasive biological samples, namely saliva and exhaled breath. Our board based OEGFET aptasensor effectively correlates transduction and signal production to biomolecule concentration. In addition, integrating our MIP EIS biosensors onto the PCB produced a portable multianalyte analysis prototype that can differentiate between concentrations of cortisol spiked saliva samples and 8-isoprostane spiked EBCs. The integrated soft-fluidic microchannels in both sensors allow for simple sample handling, which combined with the applicability of the platform to other salivary hormones, makes this a promising step towards a fully integrated biological fluid analysis panel for non-invasive biological samples. The reported OEGFET aptasensor linear detection range covers the physiological saliva reference ranges (tested 273 µM to 2.73 pM) with linearity comparable to the lab bench equipment data with reasonably high sensor resolutions. The MIP EIS biosensor board-based test demonstrated the expected impedance features, but with 210% increase in the collected impedance values. The demonstrated system-on-board configuration is the first prototype in the path to development of a low footprint, low power (<300 mW), portable, sample-to-answer PoC device for non-invasive, real-time and/or on-demand quantification of multiple biochemical analytes.

V. Acknowledgements

The authors acknowledge financial support from the Natural Science and Engineering Research Council (NSERC) Canada. The authors are thankful to Rob Vandusen and Angela Mccormick of the Carleton Microfab Facility for fabrication assistance.

VI. References

[1] S.R. Bornstein et al., “Diagnosis and treatment of primary adrenal insufficiency: An Endocrine Society clinical practice guideline.” *Journal of Clinical Endocrinology & Metabolism*. vol, 101, no. 2, pp.364-89, 2016.

[2] K.A. Smith, J. Shepherd, A. Wakil, and E.S. Kilpatrick. “A comparison of method for the measurement of 8-isoPGF2a: A Marker of Oxidative Stress”. *Annals of Clinical Biochemistry.* Vol. 48, no. 2, pp. 147-154, 2010.

[3] N.M. Grob, M. Aytekin, and R.A. Dweik. “Biomarkers in exhaled breath condensate: a review of collection, processing and analysis”. *Journal of breath research*, vol. 3, no. 2, art no. 037004, 2008.

[4] M. Gröschl.. “Saliva: A reliable sample matrix in bioanalytics”. *Bioanalysis*. 9, 2017, 10.4155/bio-2017-0010.

[5] D. Narang, M. Kaur, S. Shishodiya, and F. Khan. “Saliva as a Medium: A new tool in diagnosis.” *Int J Res Health Allied Sci,* vol. 3, no. 4, pp. 56-58, 2018.

[6] M. Gröschl. "Current status of salivary hormone analysis." *Clinical chemistry* 54, no. 11 (2008): 1759-1769.

[7] M. Gröschl. "The physiological role of hormones in saliva." *Bioessays* 31, no. 8 (2009): 843-852

[8] C.C. Chernecky, B.J. Berger. “Cortisol - plasma or serum.” In: eds. *Laboratory Tests and Diagnostic Procedures*. 6th ed. St Louis, MO: Elsevier Saunders; 2013:388-389.

[9] C. Sun, Y. Wang, M. Sun, Y. Zou, C. Zhang, S. Cheng, and W. Hu. "Facile and cost-effective liver cancer diagnosis by water-gated organic field-effect transistors." *Biosensors and Bioelectronics*. vol. 164, art. no. 112251, 2020.

[10] R. Massey, R. Prakash. “Modeling the Double Layer Capacitance Effect in Electrolyte Gated FETs with Gel and Aqueous Electrolytes”. *Micromachines*. vol. *12*, art. no 1569, 2021.

[11] R. Massey, R. Prakash, “Flexible Organic Electrolyte Gated FET Biosensor with Integrated Soft Fluidics for Cortisol Monitoring in Oral Samples*” IEEE J-FLEX*, January 2022 [in press].

[12] R. Massey, Prakash R. "Flexible Organic Electrolyte Gated FET Biosensor with Integrated Soft Fluidics for Cortisol Monitoring in Oral Samples." in *2021 IEEE Sensors, Sydney Australia*

[13] R. Selvaraj, N.J. Vasa, S.M.S. Nagendra, B. Mizaikoff, “Advances in Mid-Infrared Spectroscopy-Based Sensing Techniques for Exhaled Breath Diagnostics”. *Molecules*. vol. *25*, pp. 2227, 2020 https://doi.org/10.3390/molecules25092227

[14] L. Prest, “Fundamental investigation of fuel cell-based breath alcohol sensors and the cause of sensor degradation in low-humidity conditions”. Diss. UOIT, 2011.

[15] M.D. Davis, S.J Fowler, and A.J. Montpetit. “Exhaled breath testing–a tool for the clinician and researcher”. *Paediatric respiratory reviews*, vol. 29, pp.37-41, Feb 2019.

[16] A. Vasilescu, B. Hrinczenko, G.M. Swain and S.F. Peteu, “Exhaled breath biomarker sensing.” *Biosensors and Bioelectronics*, vol. 182, p.113193, June 2021.

[17] D. Yang, R. Gopal, T. Lkhagvaa, D Choi. “Metal-oxide gas sensors for exhaled-breath analysis: a review.” *Meas. Sci. Technol.* vol 32, Art no 102004, July 2021.

[18] A.D. Wilson. "Advances in electronic-nose technologies for the detection of volatile biomarker metabolites in the human breath." *Metabolites*. 2015, vol. 5, no. 1, pp. 140-163.

[19] G.E. Carpagnano, S.A. Kharitonov, O. Resta, M.P. Foschino-Barbaro, E. Gramiccioni, P.J. Barnes. “Increased 8-isoprostane and interleukin-6 in breath condensate of obstructive sleep apnea patients.” *Chest*. 2002, vol. 122, pp.1162–1167.

[20] B. Gamero, S. Bebe and R. Prakash, "Molecularly Imprinted Electroimpedance Sensor for Detection of 8-Isoprostane in Exhaled Breath Condensate," in *IEEE Sensors Letters*, vol. 5, no. 9, pp. 1-4, Sept. 2021, Art no. 4500404, doi: 10.1109/LSENS.2021.3103433.

[21] J. J. BelBruno, “Molecularly Imprinted Polymers,” *Chemical Reviews*, vol. 119, no. 1, pp. 94–119, 2018.

[22] D. Refaat, M. G. Aggour, A. A. Farghali, R. Mahajan, J. G. Wiklander, I. A. Nicholls, and S. A. Piletsky, “Strategies for Molecular Imprinting and the Evolution of MIP Nanoparticles as Plastic Antibodies—Synthesis and Applications,” *International Journal of Molecular Sciences*, vol. 20, no. 24, p. 6304, 2019.

[23] K. Smolinska-Kempisty et al., “A comparison of the performance of molecularly imprinted polymer nanoparticles for small molecule targets and antibodies in the ELISA format,” *Scientific Reports*, vol. 6, no. 1, 2016.

[24] A. A. Lahcen and A. Amine, “Recent Advances in Electrochemical Sensors Based on Molecularly Imprinted Polymers and Nanomaterials,” *Electroanalysis*, vol. 31, no. 2, pp. 188–201, 2018.

[25] D. Duan, X. Si, Y. Ding, L. Li, G. Ma, L. Zhang, and B. Jian, “A novel molecularly imprinted electrochemical sensor based on double sensitization by MOF/CNTs and Prussian blue for detection of 17β-estradiol,” Bioelectrochemistry, vol. 129, pp. 211–217, 2019.

[26] S. Gaggiotti et al., “Peptides, DNA and MIPs in Gas Sensing. From the Realization of the Sensors to Sample Analysis,” *Sensors*, vol. 20, no. 16, p. 4433, 2020.

[27] J. Martin et al., “Tunable stringency aptamer selection and gold nanoparticle assay for detection of cortisol,” *Anal. Bioanal. Chem*., vol. 406, no. 19, pp. 4637–4647, 2014

[28] P. Seshadri et al., “Low-picomolar, label-free procalcitonin analytical detection with an electrolyte-gated organic field-effect transistor based electronic immunosensor,” *Biosensors Bioelectron*., vol. 104, pp. 113–119, 2018.

[29] M. Berto et al., “EGOFET peptide aptasensor for label-free detection of inflammatory cytokines in complex fluids,” *Adv. Biosyst*., vol. 2, 2018, Art. no. 1700072.

[30] M. Debono et al., "Salivary cortisone reflects cortisol exposure under physiological conditions and after hydrocortisone", *J. Clin. Endocrinol. Metabolism*, vol. 101, no. 4, pp. 1469-1477, 2016.